Int. J. Electrochem. Sci., 13 **(2018)** 4575 – 4600, doi: 10.20964/2018.05.01

International Journal of
ELECTROCHEMICAL
SCIENCE
www.electrochemsci.org

New Synthesized Amino Acids-based Surfactants as Efficient Inhibitors for Corrosion of Mild Steel in Hydrochloric Acid Medium: Kinetics and Thermodynamic Approach

A. Fawzy[1,2*], *I. A. Zaafarany*[1], *H. M. Ali*[2,3], *M. Abdallah*[1,4]

[1] Chemistry Department, Faculty of Applied Science, Umm Al-Qura University, Makkah, Saudi Arabia
[2] Chemistry Department, Faculty of Science, Assiut University, Assiut, Egypt
[3] Chemistry Department, Faculty of Science, Aljouf University, Aljouf, Saudi Arabia
[4] Chemistry Department, Faculty of Science, Benha University, Benha, Egypt
[*]E-mail: afsaad13@yahoo.com

Received: 19 December 2017 / *Accepted:* 19 February 2018 / *Published:* 10 April 2018

Three amino acids based-surfactants, namely, sodium *N*-dodecyl asparagines (AS), sodium *N*-dodecyl histidine (HS) and sodium *N*-dodecyl tryptophan (TS) were synthesized and were investigated as corrosion inhibitors for mild steel (ST-37-2) in 0.5 M HCl at 25 ^{o}C. The methods employed in this work were weight-loss (WL), potentiodynamic polarization (PP) and electrochemical impedance spectroscopy (EIS). The useful surface active properties of the synthesized surfactants were also evaluated. The inhibition efficiencies were found to increase with the inhibitor concentration, while decrease with increasing the concentration of hydrochloric acid and temperature. Results obtained from the different techniques revealed that the inhibition efficiency increases in the following sequence: AS < HS < TS. The high inhibition efficiencies of the synthesized surfactants were declined in terms of strong adsorption of the surfactant molecules on mild steel surface and forming a protective film separating the steel surface from the corrosive acid medium. The adsorption operation was found to obey Langmuir isotherm. Thermodynamic and kinetic parameters were evaluated by adsorption theory and kinetic equations which support the mechanism of physical adsorption of the inhibitors. The polarization measurements showed that the tested surfactant molecules act as mixed-type inhibitors with anodic predominance. The mechanism of inhibition of mild steel corrosion was also suggested. Results obtained from all employed methods are consistent with each others.

Keywords: Amino acids-based surfactants, Mild steel, Corrosion, Inhibitors, Mechanism, Adsorption.

1. INTRODUCTION

Iron and its alloys are used widely in a broad field of industrial and machinery because of their good mechanical properties. Mild steel is an important alloy of iron used for different applications and

it is generally subjected to corrosion phenomenon in a number of environments especially in acid media. A considerable effort was devoted to develop more efficient, economically viable and environmentally compliant methods to prevent iron corrosion. However, using corrosion inhibitors is considered as one of the most effective, practical and economic methods to protect metallic surfaces against corrosion in aggressive media. Corrosion inhibitors are organic compounds containing heteroatoms, such as nitrogen, oxygen and sulfur, and unsaturated bonds [1-11]. The inhibitory action of these compounds is due to their adsorption on the metal surface and blocking it, and thus prevent the corrosion process to occur [12] because the adsorbed film behaves as a barrier which isolates metallic surface from the aggressive anions present in the solution. Such adsorption may has physical or chemical nature [13,14]. The long-chain carbon linkage and multiple adsorption sites of the inhibitor can block large area of the metal surface [15]. Also, the synergistic effect of some anions or cations at much lower concentrations with inhibitors can be applied [16-20], where synergism is very useful in the inhibition process.

Surfactant molecules are widely used as inhibitors for the corrosion of various metals and alloys in different media [21]. The combination of polar amino acids and different nonpolar hydrocarbon chain compounds produces amino acids-based surfactants. This type of surfactants is of great interest in the field of novel surfactant research because these surfactants have excellent surface active properties, quick biodegradation, environmentally friendly, excellent antimicrobial and antifungal activities in comparison to conventional surfactants [22]. They possess excellent emulsifying and detergency properties [23]. They have great potential to be applied in food, pharmacy and cosmetic industries [24-27]. The literature survey revealed that there are very few reports about the utilization of amino acids-based surfactants in the field of corrosion inhibition of metals and alloys [28]. For this reason, the present study aimed to evaluate the effectiveness of some new synthesized surfactants based on amino acids (illustrated in Figure 1) as corrosion inhibitors for mild steel in HCl using weight-loss, potentiodynamic polarization, electrochemical impedance spectroscopy and scanning electron microscopy. Furthermore, useful surface active properties of the synthesized surfactants will be evaluated.

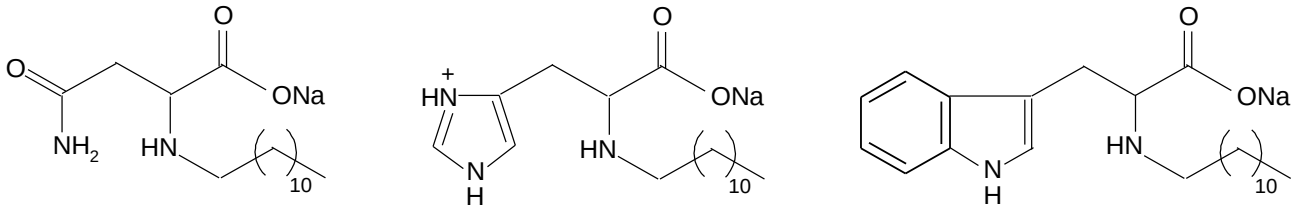

Sodium N-dodecyl asparagine (AS) Sodium N-dodecyl histidine (HS) Sodium N-dodecyl tryptophan (TS)

Figure 1. Structures of the synthesized amino acids-based surfactants.

2. EXPERIMENTAL

2.1. Materials

All solutions employed in this work were freshly prepared from Merck or Aldrich chemicals using bidistilled water. Stock solutions of the corrosive medium (HCl) were prepared by dilution of 37% HCl (Merck) using bidistilled water. The new surfactant inhibitors were synthesized as reported earlier [29,30]. The concentration range of the synthesized surfactants (inhibitors) used was 100-900 ppm (mg l^{-1}). Other reagent solutions were prepared by dissolving the required amounts of the samples in bidistilled water and the desired concentrations were obtained by appropriate dilution. Each experiment was carried out in aerated stagnant solutions and was repeated at least three times under the same conditions to check the reproducibility and the average of the three replicated values was used for further processing of the data. On the other hand, corrosion tests were performed on a cylindrical mild steel samples which has chemical composition (wt%): 0.070 C, 0.070 Si, 0.290 Mn, 0.012 S, 0.021 P, and the remainder is Fe.

2.2. Weight-Loss Measurements

Weight loss measurements were performed in a temperature-controlled system. The volume of the corrosive media was 100 ml. The mild steel samples employed for weight loss measurements were cylindrical rods of areas closed to 14 cm^2. These rods were first mechanically polished using SiC papers (emery papers) in successive grades from 200 to 1200, and then washed with distilled water and acetone. After weighing accurately, the mild steel samples were immersed in the corrosive media (in absence and presence of different concentrations of the inhibitors) and at different temperatures in 250 ml beakers. After 6 h, the mild steel samples were taken out, washed, dried and weighed accurately. Then, the average weight loss of at least three parallel mild steel samples, in each experiment, could be obtained. The corrosion rate (CR) was calculated in mils penetration per year (mpy) from the following equation [31]:

$$\text{CR (mpy)} = \frac{KW}{Atd} \qquad (1)$$

where K is a constant equals 3.45 x 10^6, W is the weight loss in grams, A is the specimen area in cm^2, t is time in hour and d is the density of mild steel (7.86 g/cm^3). The inhibition efficiency (% IE) and the degree of surface coverage (θ) of the synthesized surfactants on the corrosion of mild steel were calculated as follows [32]:

$$\% \text{ IE} = \theta \text{ x } 100 = \left[1 - \frac{CR_{inh}}{CR}\right] \text{ x } 100 \qquad (2)$$

where CR and CR_{inh} are corrosion rate values without and with inhibitor, respectively.

2.3. Electrochemical Measurements

Both electrochemical measurements, potentiodynamic polarization (PP) and electrochemical impedance spectroscopy (EIS), were performed using temperature-controlled PGSTAT30 potentiostat/galvanostat in a three-electrode cell with a Pt counter electrode (CE), a $Hg/Hg_2SO_4/SO_4^{2-}$ coupled to a fine Luggin capillary as a reference electrode (RE) and the working electrode (WE) which had the form of rod from the investigated mild steel sample. The cylindrical mild steel sample was pressed into a Teflon holder and the exposed electrode area to the corrosive solution was 0.5 cm^2. Before each experiment the WE was treated as in weight-loss measurements, then it was inserted immediately into the glass cell that contained 100 ml of the corrosive medium (blank) and the required inhibitor concentration at open circuit potential (OCP) for about 60 min. or until a steady state was attained. Potentiodynamic polarization curves were obtained by changing the electrode potential automatically at a scan rate of 2.0 mV/s which repeated about three times to test the results reproducibility. Also, the values of % IE and θ of the synthesized surfactants can be calculated from the following relation:

$$\% \text{ IE} = \theta \text{ x } 100 = \left[1 - \frac{i_{corr(inh)}}{i_{corr}}\right] \text{ x } 100 \qquad (3)$$

where, i_{corr} and $i_{corr(inh)}$ are corrosion current densities in the absence and presence of the inhibitor, respectively. The values of corrosion current densities were determined by extrapolation of the slopes of cathodic and anodic Tafel lines (β_c, β_a), of the polarization curves, to the corrosion potentials.

EIS measurements were performed in a frequency range of 100 kHz to 0.1 Hz with an amplitude of 4.0 mV peak-to-peak using AC signals at OCP. % IE was calculated from the charge transfer resistance (R_{ct}) using the following equation [33]:

$$\% \text{ IE} = \left[1 - \frac{R_{ct}}{R_{ct(inh)}}\right] \text{ x } 100 \qquad (4)$$

where R_{ct} and $R_{ct(inh)}$ are the charge transfer resistance values (in ohms cm^2) without and with inhibitor, respectively. R_{ct} is a measurement of electron transfer across the electrode surface.

2.4. Surface Investigations

Scanning electron microscopy (SEM) experiments were carried out in order to investigate the morphology of mild steel surface before and after addition of the synthesized surfactants to verify if these surfactants are adsorbed on steel surface or just peeled off it.

2.5. Evaluation of Surface Active Properties of the Synthesized Surfactants

Surface active properties are very important for any synthesized surfactant. In the present study, we aimed to examine any structure–property relationship with respect to the change in the amino acid head group. Some useful surface active properties for each surfactant were evaluated.

Surface tension measurements were carried out by preparing different concentrations of synthesized surfactants solutions in bidistilled water, thermostated at 25 ^{o}C and measuring their surface tension values using a Tensiometer equipped with a platinum ring. Other useful properties of the synthesized surfactants such as cloud points, foaming heights and wetting times were also evaluated and discussed.

3. RESULTS AND DISCUSSION

3.1. Weight-Loss Measurements and Effect of Temperature

3.1.1. Effect of Acid Concentration on the Corrosion Rate

Figure 2 displays the relation between the weight loss and immersion time for mild steel in different concentrations of HCl solutions in the range of (0.1 – 1.0 M) at a temperature of 25 ^{o}C. The values of the corrosion rates measured in mpy are listed in Table 1. The results indicated that the corrosion rate of mild steel was found to increase with increasing the concentration of the corrosive medium (HCl solutions.

Also, the effect of HCl concentration in the presence of a constant concentration of the synthesized surfactants, namely 500 ppm, on the inhibition efficiency of mild steel is shown in Figure 3. From Figure 3, it is clear that inhibition efficiency decreased with increasing HCl concentration indicating that the synthesized inhibitors are more effective at low concentration of HCl (0.1 M).

Table 1. Corrosion rates (CR) in mpy for mild steel in different concentrations of HCl solutions.

[HCl], M	0.1	0.3	0.5	0.7	1.0
CR (mpy)	137	144	162	173	184

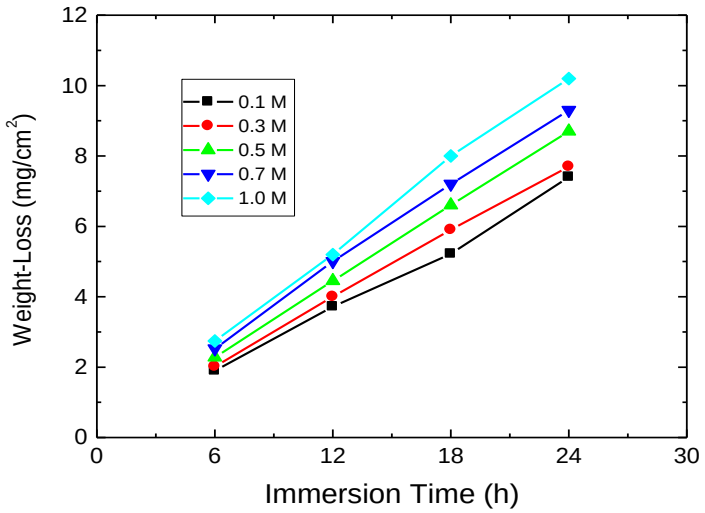

Figure 2. Weight-loss versus immersion time for mild steel in different concentrations of HCl solutions at 25 ^{o}C.

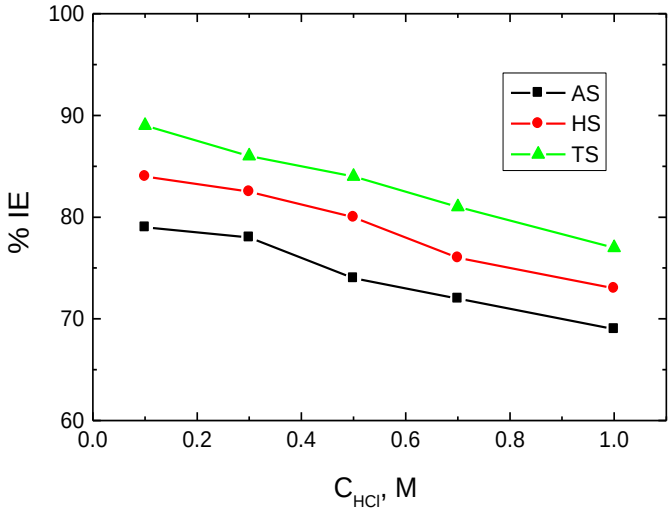

Figure 3. Effect of concentration of HCl solution on the inhibition efficiencies of 500 ppm of the synthesized surfactants for the corrosion of mild steel at 25 ^{o}C.

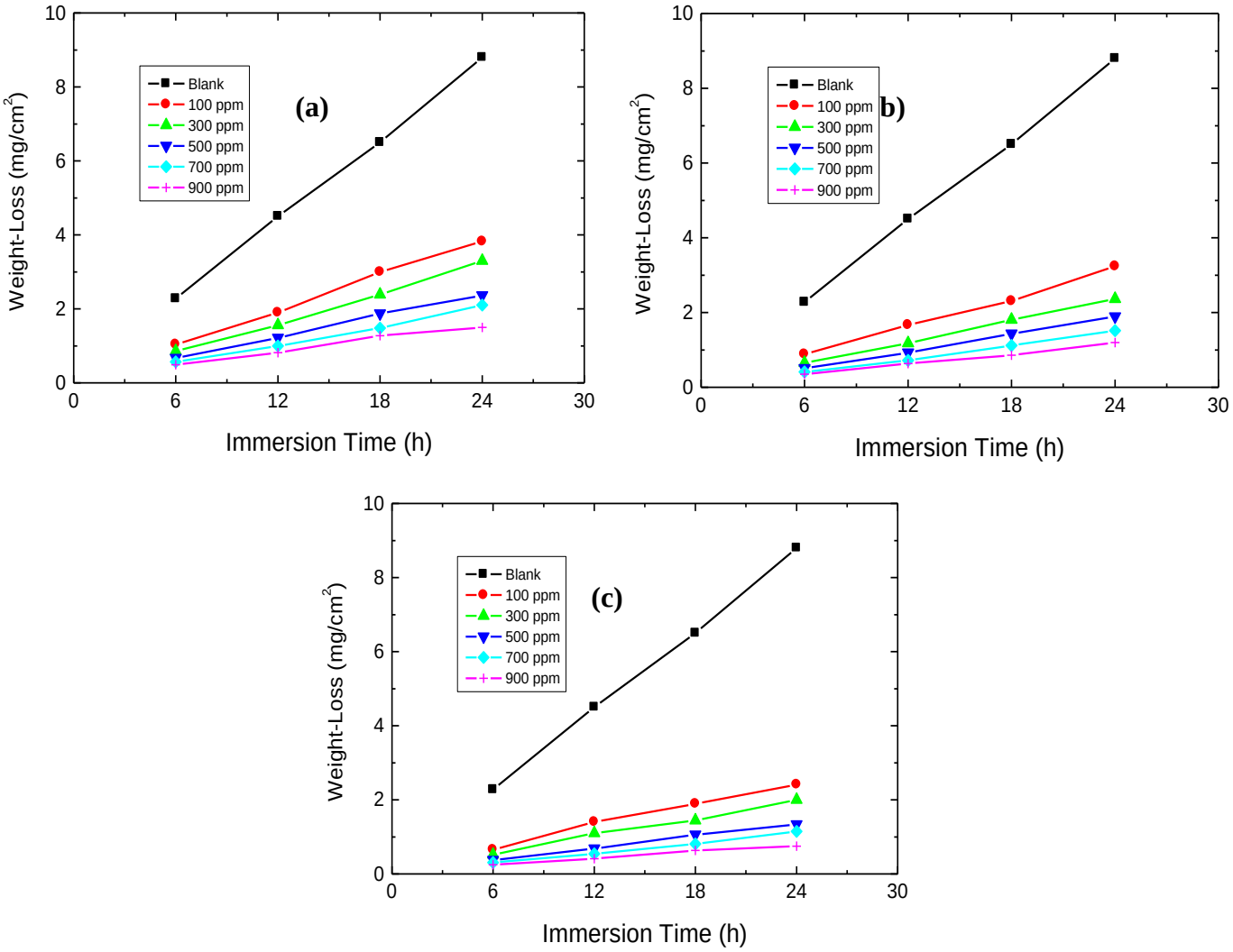

Figure 4(a-c). Weight-loss versus immersion time for mild steel in 0.5 M HCl solution in the absence and presence of different concentrations of the synthesized surfactants at 25 ^{o}C. (a) AS, (b) HS and (c) TS.

3.1.2. Effect of Added Synthesized Surfactants on the Corrosion Rate

WL experiments of mild steel in 0.5 M HCl solution were performed in the absence and presence of various concentrations of the surfactants (100 – 900 ppm) at different temperatures (15, 25, 35 and 45 ^{o}C); only the WL versus time curves obtained at 25 ^{o}C are shown here, Figure 4(a-c). Values of CR, θ and %IE of the surfactants are also listed in Table 2. It is obvious from Table 2 that for all synthesized surfactants, that CR values get decreased and %IE increased with the inhibitors concentrations. These results lead to the conclusion that these synthesized surfactants are efficient as inhibitors for mild steel dissolution in 0.5 M HCl solution. The order of inhibition efficiencies is as follows: AS < HS < TS.

3.1.3. Effect of Immersion Time on the Inhibition Efficiencies

The effect of immersion time on the inhibition efficiencies of a concentration of 500 ppm of the synthesized surfactants in 0.5 M HCl solution was investigated for 3 to 36 h at 25 ^{o}C and is illustrated in Figure 5. This figure showed that the surfactant molecules inhibit the corrosion of mild steel for all immersion times. At first stages, the inhibition efficiencies increase greatly with increasing the immersion time up to about 12 h, then decrease slightly with further small elapse of time and finally reach the constant values after more than 20 h. Increasing inhibition efficiencies with immersion time at first stages can be attributed to the adsorption of multi layers of the inhibitor molecules on the mild steel surface which causes more inhibition efficiencies. After about 12 h, some adsorbed inhibitor molecules are believed to leave mild steel surface causing a decrease in the effective area covered by such molecules to some extent leading to slight decreasing of the inhibition efficiencies. After 20 h, the change in inhibition efficiencies with immersion time is negligible. This means that, the adsorbed films become more compact on the surface of mild steel, and then becomes more stable [34,35]. This indicates that the synthesized surfactants are efficient corrosion inhibitors for mild steel in 0.5 M HCl.

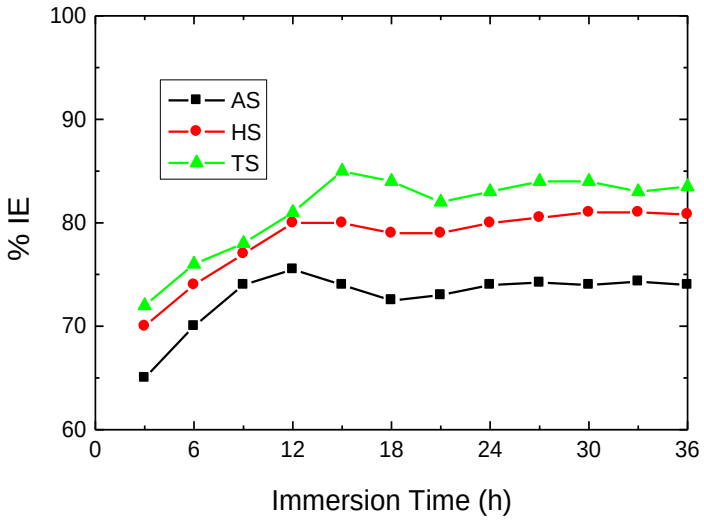

Figure 5. Variation of inhibition efficiencies with immersion time for mild steel in 0.5 M HCl containing 500 ppm of the synthesized surfactants at 25 ^{o}C.

3.1.4. Effect of Temperature

The effect of temperature on the corrosion rate of mild steel in 0.5 M HCl and on the inhibition efficiencies of the synthesized surfactants at different concentrations has been investigated in the temperature range of (15 – 45 ^{o}C) using weight-loss measurements. Similar curves of Figure 4 were obtained but not shown. With rising temperature, the rates of corrosion increase and %IE of the additives decrease as listed in Table 2. The observed decrease in %IE as the temperature increases suggests that physical adsorption is the predominant mechanism [36,37]. Generally the increase in temperature usually accelerates the hydrogen gas evolution in an acid medium and reduces inhibitor adsorption resulting in acceleration of the dissolution process on mild steel surface. However, at higher concentration of the inhibitors, increase in temperature had very little effect on the corrosion rates.

Table 2. Corrosion rates (CR) in mpy of mild steel, degrees of surface coverage (θ) and inhibition efficiencies (% IE) of the synthesized surfactants with different concentrations in 0.5 M HCl solution at different temperatures.

0.5 M HCl +	Inhibitors Concn. (ppm)	Temperature (^{o}C)											
		15			25			35			45		
		CR	% IE	θ	CR	% IE	θ	CR	% IE	θ	CR	% IE	θ
--	**0**	**146**	--	--	**162**	--	--	**179**	--	--	**194**	--	--
AS	**100**	62	57	0.57	72	55	0.55	85	52	0.52	104	46	0.46
	300	51	65	0.65	58	64	0.64	69	61	0.61	82	58	0.58
	500	35	76	0.76	42	74	0.74	50	72	0.72	60	69	0.69
	700	28	81	0.81	34	79	0.79	42	76	0.76	49	74	0.74
	900	22	85	0.85	29	82	0.82	36	80	0.80	45	77	0.77
HS	**100**	47	68	0.68	56	65	0.65	69	61	0.61	82	58	0.58
	300	35	76	0.76	44	73	0.73	55	69	0.69	65	66	0.66
	500	27	82	0.82	32	80	0.80	41	77	0.77	49	74	0.74
	700	20	86	0.86	24	85	0.85	29	84	0.84	38	80	0.80
	900	16	89	0.89	20	88	0.88	24	86	0.86	33	83	0.83
TS	**100**	34	76	0.76	45	72	0.72	56	69	0.69	64	66	0.66
	300	28	81	0.81	35	78	0.78	45	75	0.75	54	72	0.72
	500	20	86	0.86	26	84	0.84	37	80	0.80	42	78	0.78
	700	15	90	0.90	20	88	0.88	29	84	0.84	33	83	0.83
	900	12	92	0.92	16	90	0.90	21	87	0.87	27	86	0.86

3.1.5. Adsorption Isotherm

For testing the adsorption isotherm of the investigated inhibitors obeyed by this system, the plots of fractional surface coverage values (C_{inh}/θ) versus inhibitor concentrations (C_{inh}) at all the studied temperatures were drawn. Straight lines with almost unit slopes and correlation coefficients of ($0.989 \leq R^2 \leq 0.997$) were obtained as illustrated in Figure 6(a-c) indicating that the adsorption of the investigated inhibitors on mild steel surface in HCl solution agrees with the Langmuir adsorption isotherm which is given by following equation [38]:

$$\frac{C_{inh}}{\theta} = \frac{1}{K_{ads}} + C_{inh} \quad (5)$$

where K_{ads} is the equilibrium constant of the adsorption process which are listed in Table 3. This Table showed that the values of K_{ads} decrease with increasing temperature indicating strong adsorption of the surfactants on mild steel surface at relatively lower temperature, but upon raising temperature, the adsorbed surfactants tend to desorb from the steel surface.

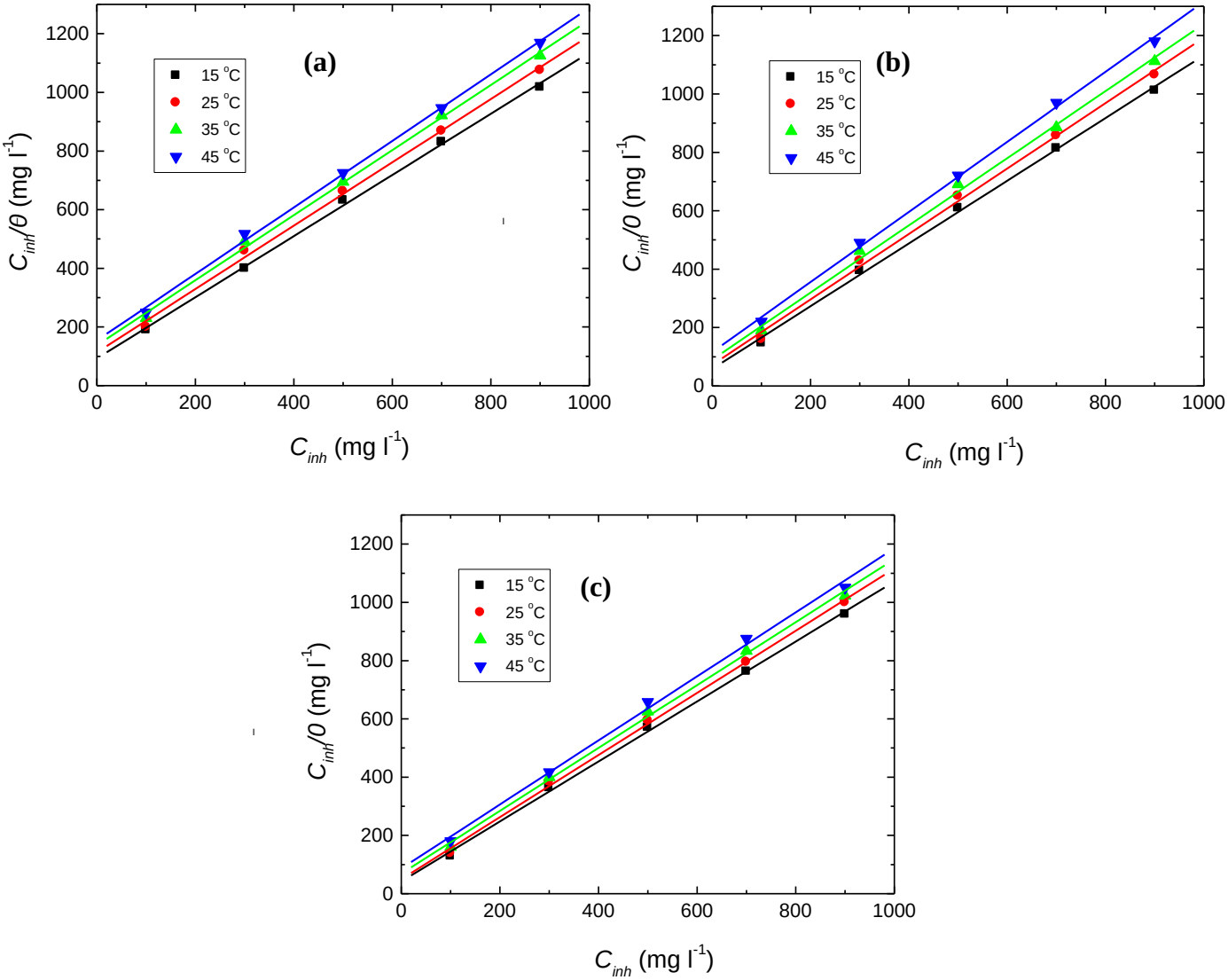

Figure 6(a-c). Langmuir adsorption isotherms for the synthesized surfactants adsorbed on mild steel surface in 0.5 M HCl solution at different temperatures. (a) AS, (b) HS and (c) TS.

3.1.6. Thermodynamic Parameters

Thermodynamic parameters can provide valuable information about the mechanism of corrosion inhibition. The standard free energy of adsorption (ΔG^{o}_{ads}) is related to K_{ads} according to the following equation [39],

$$\Delta G^{o}_{ads} = -RT \ln(55.5\, K_{ads}) \quad (6)$$

where, R is the universal gas constant and the value 55.5 is the molar concentration of water in solution in mol l^{-1}. The values of (ΔG^{o}_{ads}) for the three studied inhibitors were calculated at different temperatures and are listed in Table 3. The high values of (ΔG^{o}_{ads}) obtained for the surfactant TS indicated that this compound is more strongly adsorbed on steel surface in 0.5 M HCl than the other surfactants. This is in a good agreement with the values of %IE of the investigated surfactants obtained from all employed techniques.

On the other hand, it has been reported [40,41] that values of ΔG^{o}_{ads} around -20 kJ mol^{-1} or lower are consistent with physisorption where an electrostatic interaction between the active positive charge on iron surface and negative charge on chloride ion. While those more negative than -40 kJ mol^{-1} involve charge sharing or transfer from the inhibitor molecules to the metal surface to form a coordinate bond between the surfactant molecules and the vacant d-orbital of iron (chemisorption). The obtained ΔG^{o}_{ads} values indicated that the adsorption mechanism of the synthesized surfactants on mild steel in 0.5 M HCl solution is a mixed from physical and chemical adsorption [41].

The standard adsorption heat (ΔH^{o}_{ads} / kJ mol^{-1}) can be calculated according to the Van't Hoff equation [42]:

$$\ln K_{ads} = \frac{-\Delta H^{o}_{ads}}{RT} + \text{Constant} \quad (7)$$

The plots of ln K_{ads} vs. 1/T gave good straight lines with slopes of $-\Delta H^{o}_{ads} / R$ as illustrated in Fig. 7, thus the values of $-\Delta H^{o}_{ads}$ were obtained and are presented in Table 3.

Endothermic adsorption process ($\Delta H^{o}_{ads} > 0$) is attributed to chemisorption [43], an exothermic adsorption process ($\Delta H^{o}_{ads} < 0$) may involve either physisorption or chemisorption or a mixture of both processes. Generally, when the enthalpy values are less than or around 40 kJ mol^{-1}, the adsorption process is physisorption while in case of the values more than 100 kJ mol^{-1}, the adsorption of inhibitor follows the chemisorptions process [44]. The obtained negative values of ΔH^{o}_{ads} reveal that the adsorption of inhibitors molecules is an exothermic process with a physical nature (physisorption).

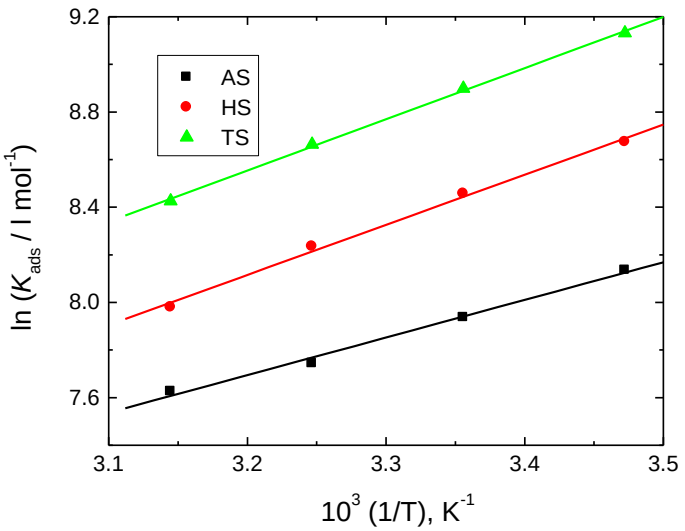

Figure 7. Van't Hoff plots for the synthesized surfactants adsorbed on mild steel surface in 0.5 M HCl.

Table 3. Values of thermodynamic parameters and adsorptive equilibrium constant (K_{ads}) for the corrosion of mild steel in 0.5 M HCl solution in the presence of different concentrations of the synthesized surfactants at different temperatures.

0.5 M HCl +	**Temp. (^{o}C)**	**10^{-3} K_{ads} l mol^{-1}**	**ΔG^o_{ads} kJ mol^{-1}**	**ΔH^o_{ads} kJ mol^{-1}**	**$\Delta S^o_{ads\ (298)}$ J mol^{-1} K^{-1}**
AS	**15**	3.41	-30.1	-13.14	56.9
	25	2.80	-29.6		55.3
	35	2.31	-29.1		53.7
	45	2.05	-28.8		52.7
HS	**15**	5.84	-31.4	-17.46	46.9
	25	4.70	-30.9		45.1
	35	3.77	-30.4		43.9
	45	2.92	-29.7		41.1
TS	**15**	9.24	-32.6	-17.88	49.3
	25	7.32	-32.0		47.4
	35	5.79	-31.4		45.4
	45	4.56	-30.8		41.7

The standard adsorption entropy (ΔS^o_{ads} / J mol^{-1} K^{-1}) can be obtained from the following rearranged Gibbs–Helmholtz equation:

$$\Delta G^o_{ads} = \Delta H^o_{ads} - T\Delta S^o_{ads} \quad (8)$$

The calculated values of ΔS^o_{ads} are listed in Table 3. The obtained positive values of ΔS^o_{ads} showed the increased randomness at the metal/solution interface during the adsorption of inhibitor molecules on mild steel surface. This increase of disorder is due to more water molecules may desorbed from the metal surface by inhibitors molecules [45].

3.1.7. Kinetic-Thermodynamic Parameters

The dependence of CR on temperature is expressed by Arrhenius equation as follows [46]:

$$\ln CR = \ln A - \frac{E_a^*}{RT} \quad (9)$$

where, E_a^* is the apparent activation energy of the corrosion process and A is the Arrhenius pre-exponential constant. It has been reported [47,48] that there are several cases regarding the effect of an inhibitor on the activation energy and inhibition efficiency; the first case is decreasing inhibition efficiency with increasing temperature, and the value of E_a^* is higher in the presence of the inhibitor compared with the blank. The second case is the reverse to case one, i.e., increasing the inhibition efficiency with temperature and E_a^* in the presence of the inhibitor is lower compared with the blank. The third one is independence of inhibition efficiency on temperature and E_a^* values in the absence and presence of inhibitor are the same.

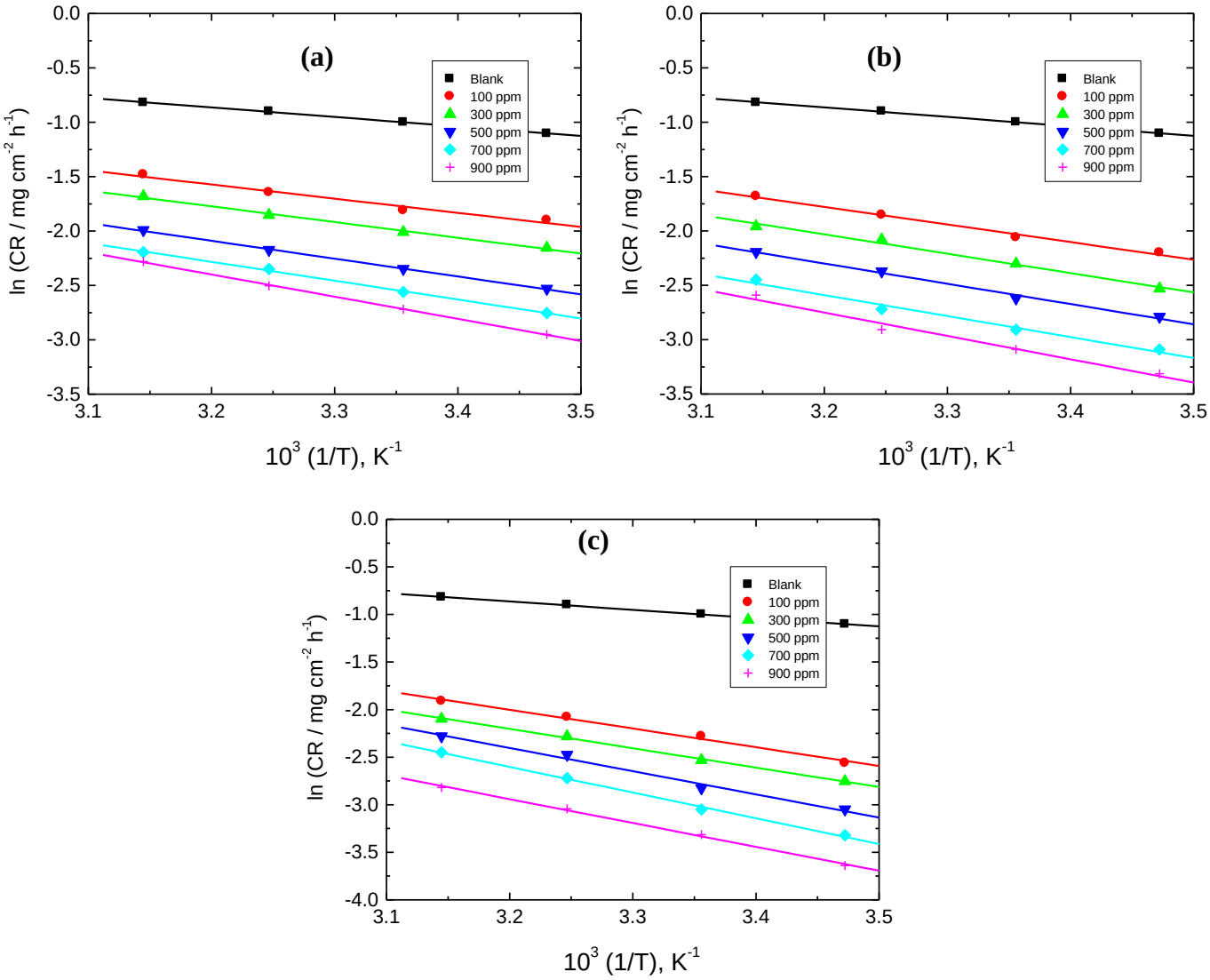

Figure 8(a-c). Arrhenius plots for the corrosion of mild steel in 0.5 M HCl solution in the absence and presence of different concentrations of the synthesized surfactants. (a) AS, (b) HS and (c) TS.

In the present study, Fig. 8(a-c) represents the Arrhenius plots (ln CR vs. 1/*T*) for mild steel in 0.5 M HCl in the absence and presence of different concentrations of the synthesized surfactants. The linear regression coefficients of all plots are higher than 0.99 indicating the validity of the used kinetic model. The values of E_a^* was computed from the slopes of the straight lines and are listed in Table 4. Inspection of the data presented in Table 4 showed that the activation energies obtained in the presence of the synthesized surfactants are higher than that in blank solution. This behavior confirmed that the above mentioned first case was attained in our study, where the values of inhibition efficiencies of the synthesized surfactants were decreased with increasing temperature and the value of E_a^* is higher in the presence of the inhibitors compared with the blank. This proved that the surfactant molecules are adsorbed on the steel surface forming a barrier for mass and charge transfer between the steel surface and the corrosive media. Furthermore, the range of E_a^* values (10.22 – 24.11 kJ mol^{-1}) are lower than the threshold value of 80 kJ mol^{-1}, required for chemical adsorption confirming the physical adsorption

of the inhibitors [49,50]. These observations are consistent with those based on the values of both ΔG^{o}_{ads} and ΔH^{o}_{ads} confirming the validity of the obtained results.

The enthalpy of activation (ΔH^{*}) and entropy of activation (ΔS^{*}) of metal dissolution are calculated using transition state equation [51]:

$$\ln\left(\frac{CR}{T}\right) = \left(\ln\frac{R}{Nh} + \frac{\Delta S^{*}}{R}\right) - \frac{\Delta H^{*}}{R}\frac{1}{T} \qquad (9)$$

where, N is Avogadro's number (6.0225×10^{23} mol^{-1}) and h is Planck's constant (6.6261×10^{-34} Js). Plots of ln(CR/T) versus 1/T gave good straight lines with slopes equal to (ΔH^{*}/R) and intercepts of ln(R/Nh) + ΔS^{*}/R and are illustrated in Figure 9(a-c).

Table 4. Activation parameters for the corrosion of mild steel in 0.5 M HCl solution in the absence and presence of different concentrations of the synthesized surfactants.

0.5 M HCl +	**Inhibitors Concn. (mg l^{-1})**	**E_a^{*} kJ mol^{-1}**	**ΔH^{*} kJ mol^{-1}**	**ΔS^{*} J mol^{-1} K^{-1}**
--	**0**	7.3	4.8	-237.2
AS	**100**	10.5	10.5	-229.4
	300	12.0	10.9	-217.2
	500	13.6	12.1	-212.0
	700	14.4	13.1	-213.1
	900	17.1	14.6	-207.1
HS	**100**	14.1	11.7	-227.4
	300	14.8	13.4	-224.7
	500	15.5	14.2	-219.9
	700	16.1	13.9	-217.1
	900	17.8	15.4	-219.1
TS	**100**	16.3	13.8	-214.1
	300	16.9	16.1	-209.1
	500	20.2	18.7	-201.5
	700	24.1	21.5	-198.9
	900	20.8	19.5	-204.7

The calculated values of ΔH^{*} and ΔS^{*} are presented in Table 4. The positive sign of ΔH^{*} suggests that the dissolution process was endothermic. The high values and negative sign of ΔS^{*} in both absence and presence of the inhibitors implying that the activated complex in the rate-determining step represents an association rather than dissociation resulting in a decrease in disorder [52].

3.2. Open Circuit Potential Measurements

The variation of open circuit potentials (OCP) with time for mild steel was followed in aerated non-stirred 0.5 M HCl solution in the absence and presence of various concentrations of the synthesized surfactants at 25 ^{o}C. Results obtained for the surfactant AS (as a representative example) are depicted in Fig. 10. Similar results were recorded for HS and TS (data not included here). It can be

observed that E_{OCP} of mild steel in the inhibitor-free HCl solution shifts towards less negative direction and takes around 30 min. to attain the steady state. This suggests initial dissolution of the air formed oxide film and the attack has been happened on the bare metal [53]. In the presence of synthesized surfactant AS, the E_{OCP} started at relatively higher positive potentials compared with that in the absence of the inhibitor and then shifted towards more negative values and steady states occurred in shorter times, compared with the blank solution. With increasing the concentration of the inhibitor, the positive shift in E_{OCP} increases pointing to enhancement of the inhibition efficiency with concentration, where more positive potential in OCP is an indication of lower corrosion rate in acidic medium [54]. Also, the anodic shifts in E_{OCP} revealed that the inhibitor might act mainly as an anodic inhibitor. However the shifts in the values of E_{OCP} were not that much to classify the inhibitor as an anodic or cathodic one (the shifts were lower than +85 mV). Therefore the investigated synthesized surfactants can be regarded as mixed-type inhibitors with anodic predominance. This positive shifts occurred in E_{corr} suggests that the inhibitor adsorbs preferentially on the steel surface impeding the anodic sites [55]. These findings may reflect the ability of the tested surfactants to inhibit the anodic process [55].

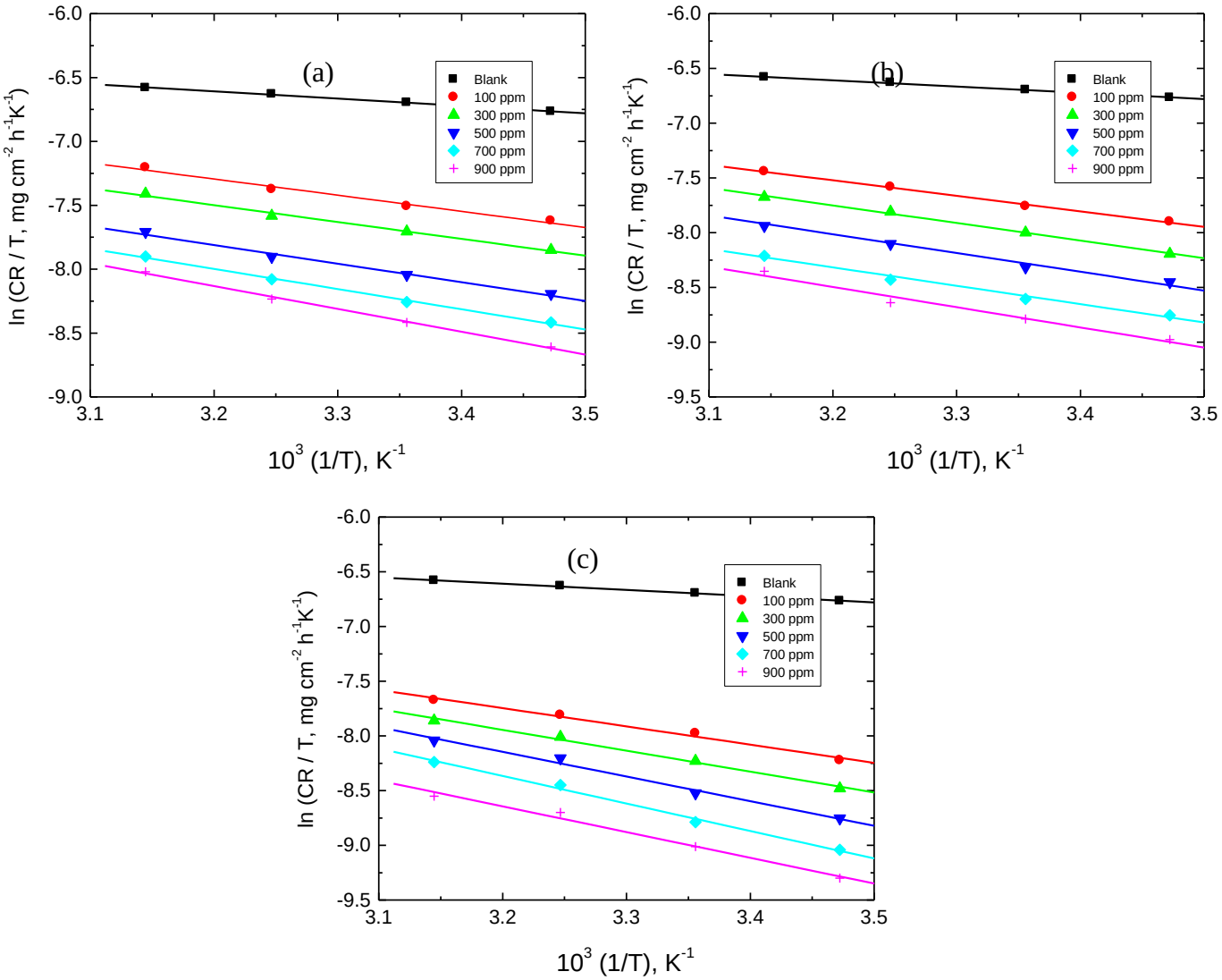

Figure 9(a-c). Transition state plots for the corrosion of mild steel in 0.5 M HCl solution in the absence and presence of the synthesized surfactants. (a) AS, (b) HS and (c) TS.

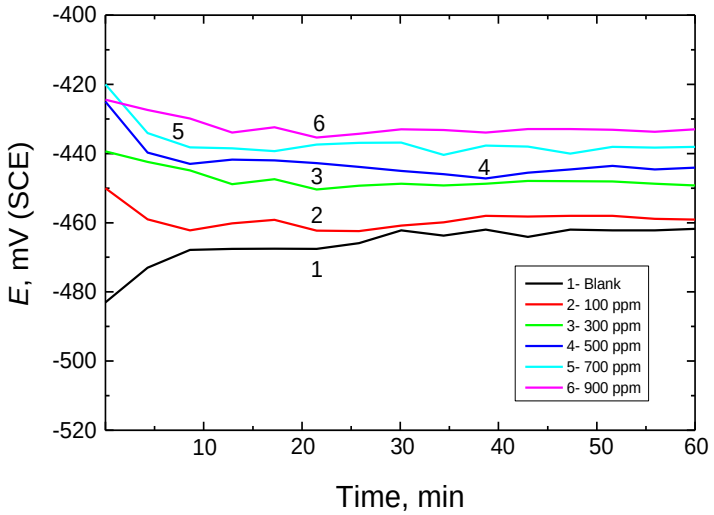

Figure 10. Variation of the OCP with time of mild steel in 0.5 M HCl solution in the absence and presence of various concentrations of the synthesized surfactant AS at 25 ^{o}C.

3.3. Potentiodynamic Polarization Measurements

3.3.1. Effect of Acid Concentration on the Corrosion Rate

Tafel plots recorded for mild steel in HCl solutions (0.1 to 1.0 M) at 25 ^{o}C are illustrated in Fig. 11. The associated corrosion parameters, i.e. corrosion potential (E_{corr}), corrosion current density (i_{corr}), cathodic and anodic Tafel slopes (β_c, β_a) were derived from polarization curve and are listed in Table 5. The data showed that the value of i_{corr} of mild steel increased with increasing acid concentration, indicating an enhancement of mild steel corrosion with acid concentration.

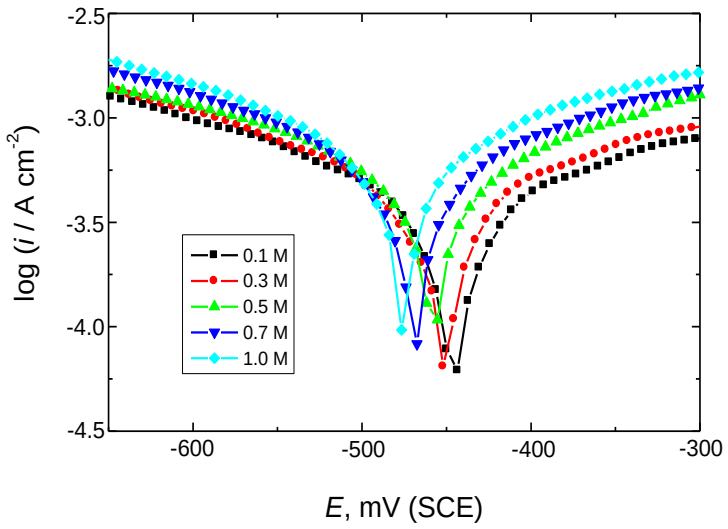

Figure 11. Potentiodynamic polarization curves for mild steel in different concentrations of HCl solutions at 25 ^{o}C.

Table 5. Polarization data for mild steel in different concentrations of HCl solutions at 25 ^{o}C.

[HCl] (mol dm^{-3})	$-E_{corr}$ (mV(SCE))	β_a (mV/decade)	$-\beta_c$ (mV/decade)	i_{corr} (μA/cm^2)
0.1	448	311	437	291
0.3	453	307	409	317
0.5	462	293	355	355
0.7	470	304	313	388
1.0	479	298	269	437

3.3.2. Effect of Added Synthesized Surfactants on the Corrosion Rate

The potentiodynamic polarization curves for mild steel in 0.5 M HCl solution in the absence and presence of the synthesized surfactants are illustrated in Fig. 12(a-c). Values of electrochemical parameters including corrosion potential (E_{corr}), i_{corr} , βc, β_a , % IE and θ were calculated from polarization curves and are listed in Table 6. From Fig. 12 and the data listed in Table 6, it can be observed that the addition of the synthesized surfactants to the blank solution (0.5 M HCl) shifted both anodic and cathodic branches of the polarization curves of mild steel in pure acid solution towards lower current density values at all investigated concentrations indicating retardation of both anodic and cathodic reactions and then inhibition of mild steel corrosion. Values of %IE increased with increasing the inhibitor concentrations and the extent of %IE of the inhibitors follow the order: AS < HS < TS. These results could be explained by the adsorption of the inhibitor molecules at the active sites of the mild steel surface, which retards both metallic dissolution and hydrogen evolution, and consequently, decreases the corrosion rate [56]. Because the inhibitors exhibited obvious anodic and cathodic inhibition effects with markedly shifting E_{corr} to more anodic potentials compared with that recorded for the blank solution, it could be concluded that the synthesized surfactants acted as mixed-type inhibitors with anodic predominance in agreement with the results obtained from OCP measurements. Also, it can observed that the surfactant TS exhibited higher efficiency more than both AS and HS.

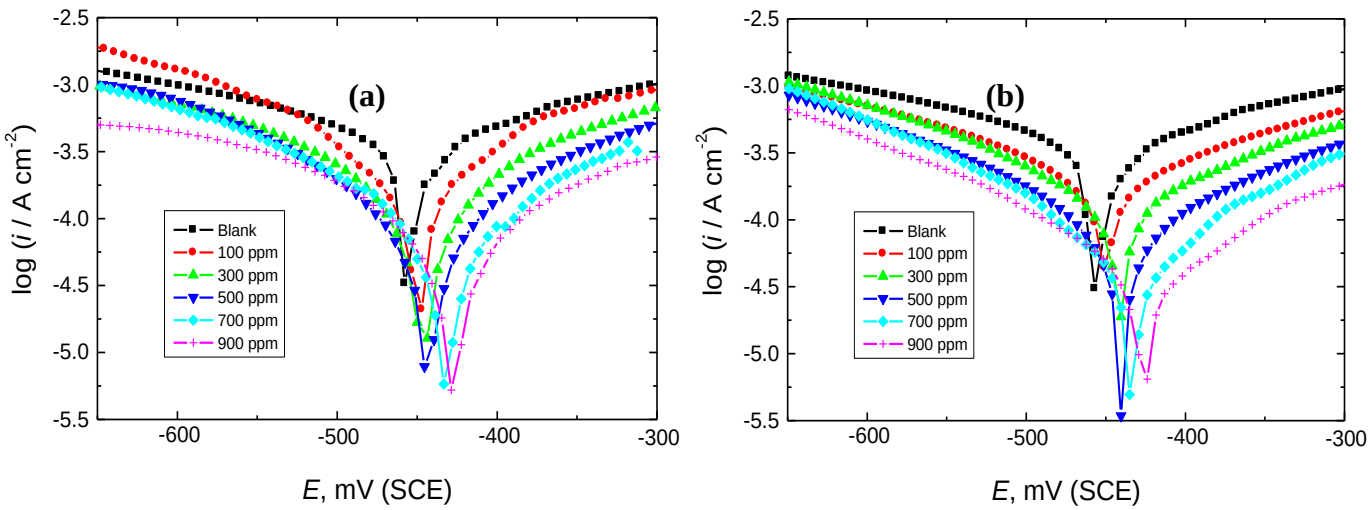

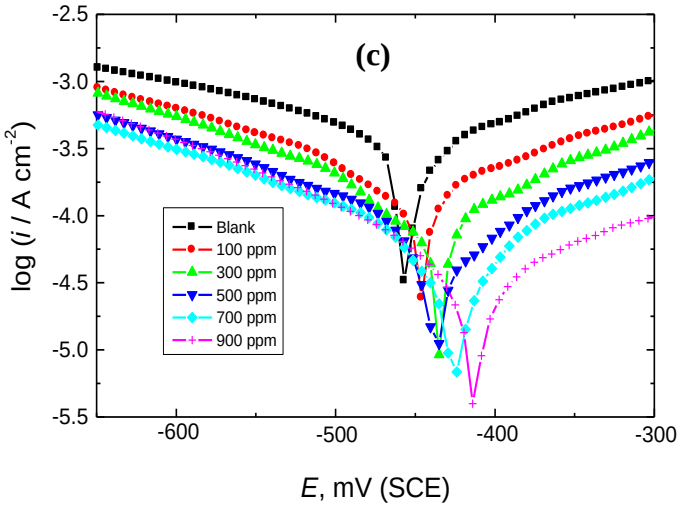

Figure 12(a-c). Potentiodynamic polarization curves for mild steel corrosion in 0.5 M HCl solution in the absence and presence of different concentrations of the synthesized surfactants at 25 ^{o}C. ((a) AS, (b) HS and (c) TS.

Table 6. Polarization data for mild steel corrosion in 0.5 M HCl solution in the absence and presence of different concentrations of the synthesized surfactants at 25 ^{o}C.

0.5 M HCl +	Inhibitors Concn. (mg/l)	$-E_{corr}$ (mV(SCE))	β_a (mV/decade)	$-\beta_c$ (mV/decade)	i_{corr} (μA/cm^2)	% IE	θ
--	0	462	293	355	355	--	--
AS	100	458	229	233	204	43	0.43
	300	449	191	227	162	54	0.54
	500	445	180	181	118	67	0.67
	700	438	153	218	82	77	0.77
	900	432	177	269	59	82	0.82
HS	100	453	251	267	171	52	0.52
	300	438	197	209	139	61	0.61
	500	439	189	194	99	72	0.72
	700	435	178	186	64	82	0.82
	900	428	164	205	58	84	0.84
TS	100	451	227	269	111	69	0.69
	300	447	198	261	87	75	0.75
	500	443	168	253	63	82	0.82
	700	426	157	244	47	87	0.87
	900	417	211	241	38	89	0.89

3.4. Electrochemical Impedance Spectroscopy Measurements

The corrosion behavior of mild steel in 0.5 M HCl solution has been also investigated in the absence and presence of the synthesized surfactants at 25 ^{o}C and after immersion of mild steel electrode in the corrosive medium for about 30 min. by the electrochemical impedance spectroscopy (EIS). Nyquist plots of mild steel corrosion in acid solutions containing various concentrations of the inhibitors are illustrated in Fig. 13(a-c). The values of R_{ct} obtained from Nyquist plots, values of %IE which calculated from the values of R_{ct} (using Eq. (4)) and values of θ are given in Table 7. It is clear from Nyquist plots that the obtained impedance spectra consist of one capacitive semicircle suggesting that adsorption of inhibitors occurs by simple surface coverage and the surfactants act as primary interface inhibitors, and the corrosion of mild steel is mainly controlled by charge transfer process [57]. The size of the capacitive semicircle of mild steel in the inhibitor-free acidic medium increased significantly after addition of the inhibitors to the corrosive medium indicating a decrease in the corrosion rate of mild steel and increasing the inhibition efficiencies, and the later were found to increase with increasing inhibitors concentrations. Also, it can be observed that the general shape of the curves is similar in the absence or presence of inhibitors of different concentrations indicating that there was no change in the corrosion mechanism [58].

It is apparent from the values of R_{ct} listed in Table 7 that the addition of inhibitors in acid medium leads to increasing the value of R_{ct} obtained in the blank solution. This indicates that the synthesized surfactants act as inhibitors via adsorption at the metal/solution interface which decreases their electrical capacities as they displace water molecules and other ions originally adsorbed on the surface [59]. Also, increasing R_{ct} value with inhibitor concentrations indicates that the amount of the inhibitor molecules adsorbed on the mild steel surface increase which form protective films on the electrode surface, and consequently become barriers to hinder the mass and charge transfer, resulting in an increase in the inhibition efficiencies [60]. With an increase in concentration of the synthesized surfactants, the protection efficiency increases which further confirms that the inhibitor acts as an efficient inhibitor for mild steel in 0.5 M HCl medium. Finally, the results of the inhibition efficiencies of the inhibitors obtained from EIS measurements were found to be in good agreement with that obtained from both PP and WL measurements as illustrated in Fig. 14(a-c).

Table 7. Values of charge transfer resistance (R_{ct}) and inhibition efficiencies (%IE) of different concentrations of the synthesized surfactants for the corrosion of mild steel in 0.5 M HCl solution at 25 ^{o}C.

Inhibitor	**AS**		**HS**		**TS**	
Concn. (ppm)	R_{ct}	**% IE**	R_{ct}	**% IE**	R_{ct}	**% IE**
0	**79**	**--**	**79**	**--**	**79**	**--**
100	149	47	184	57	239	67
300	202	61	226	65	294	73
500	293	73	304	74	395	80
700	343	77	416	81	528	85
900	376	79	527	85	658	88

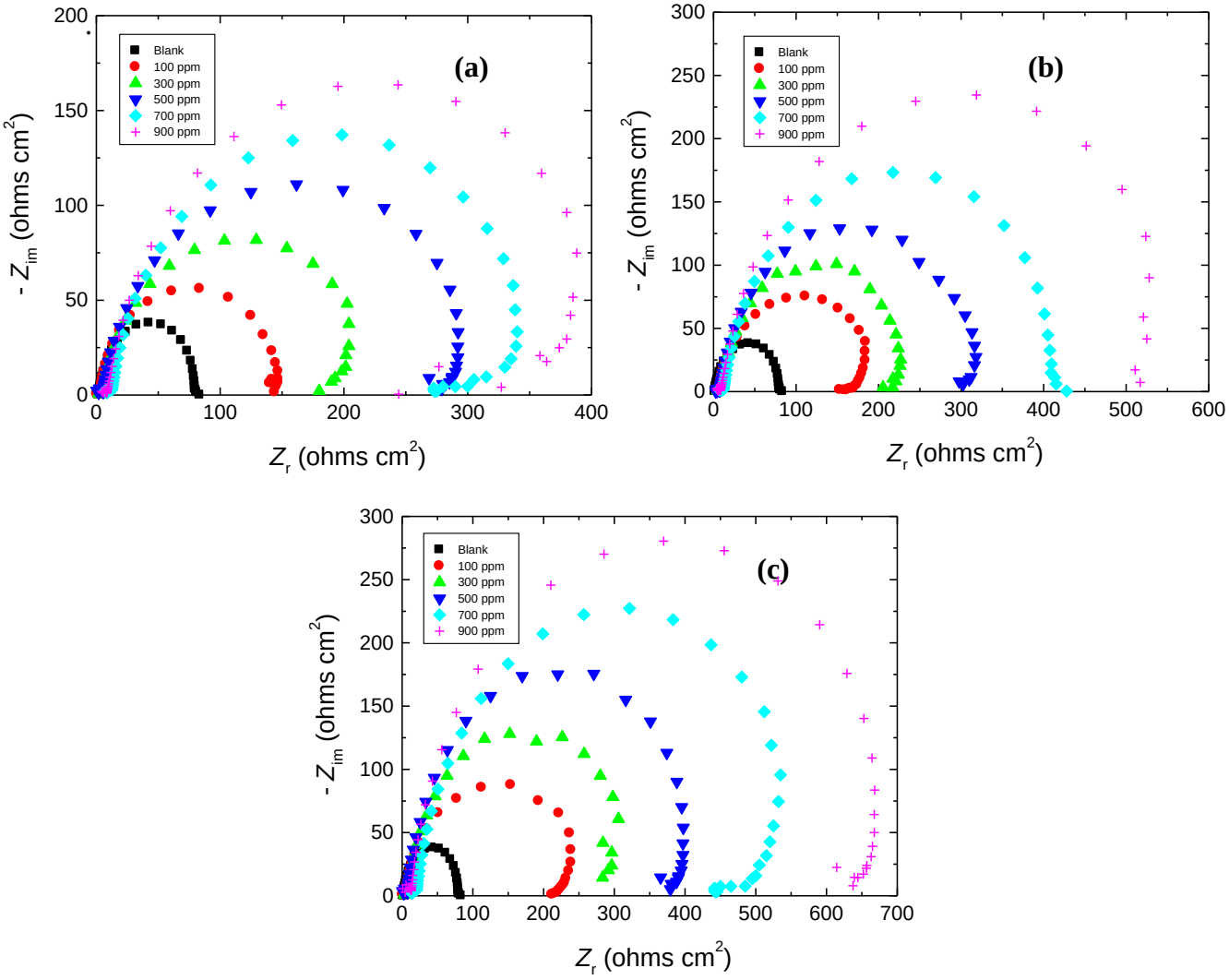

Figure 13(a-c). Nyquist plots for the corrosion of mild steel in 0.5 M HCl solution in the absence and presence of different concentrations of the synthesized surfactants at 25 ^{o}C. (a) AS, (b) HS and (c) TS.

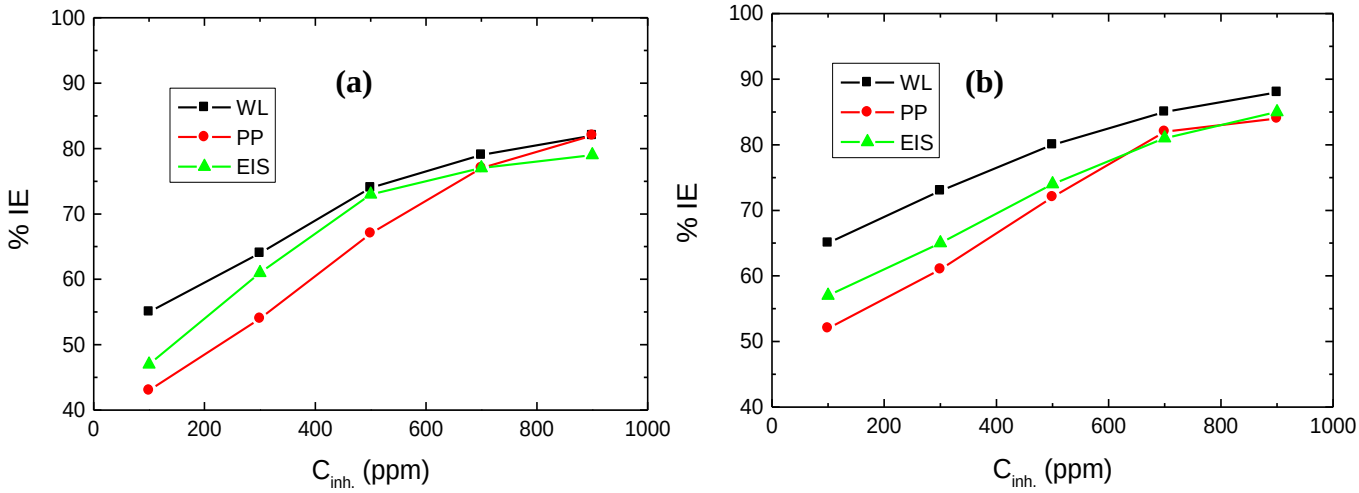

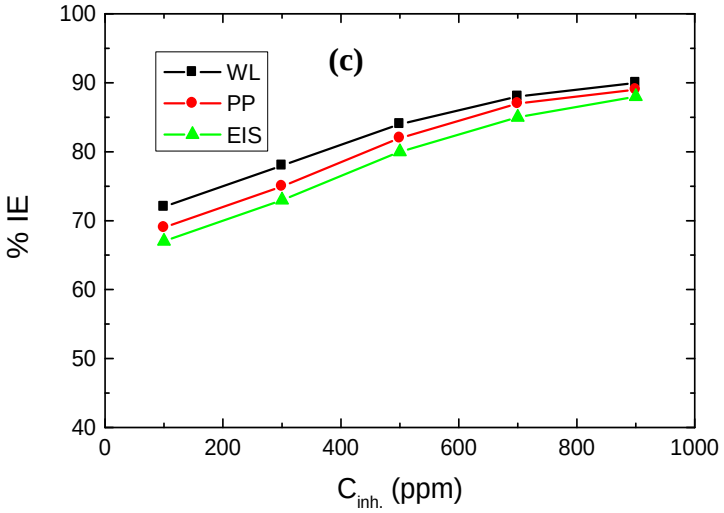

Figure 14(a-c). Comparison between the three methods employed in this work: WL, PP and EIS for the variation of the inhibition efficiencies (% IE) with the concentrations of the synthesized surfactants (C_{inh}) for the corrosion of mild steel in 0.5 M HCl at 25 ^{o}C. (a) AS, (b) HS and (c) TS.

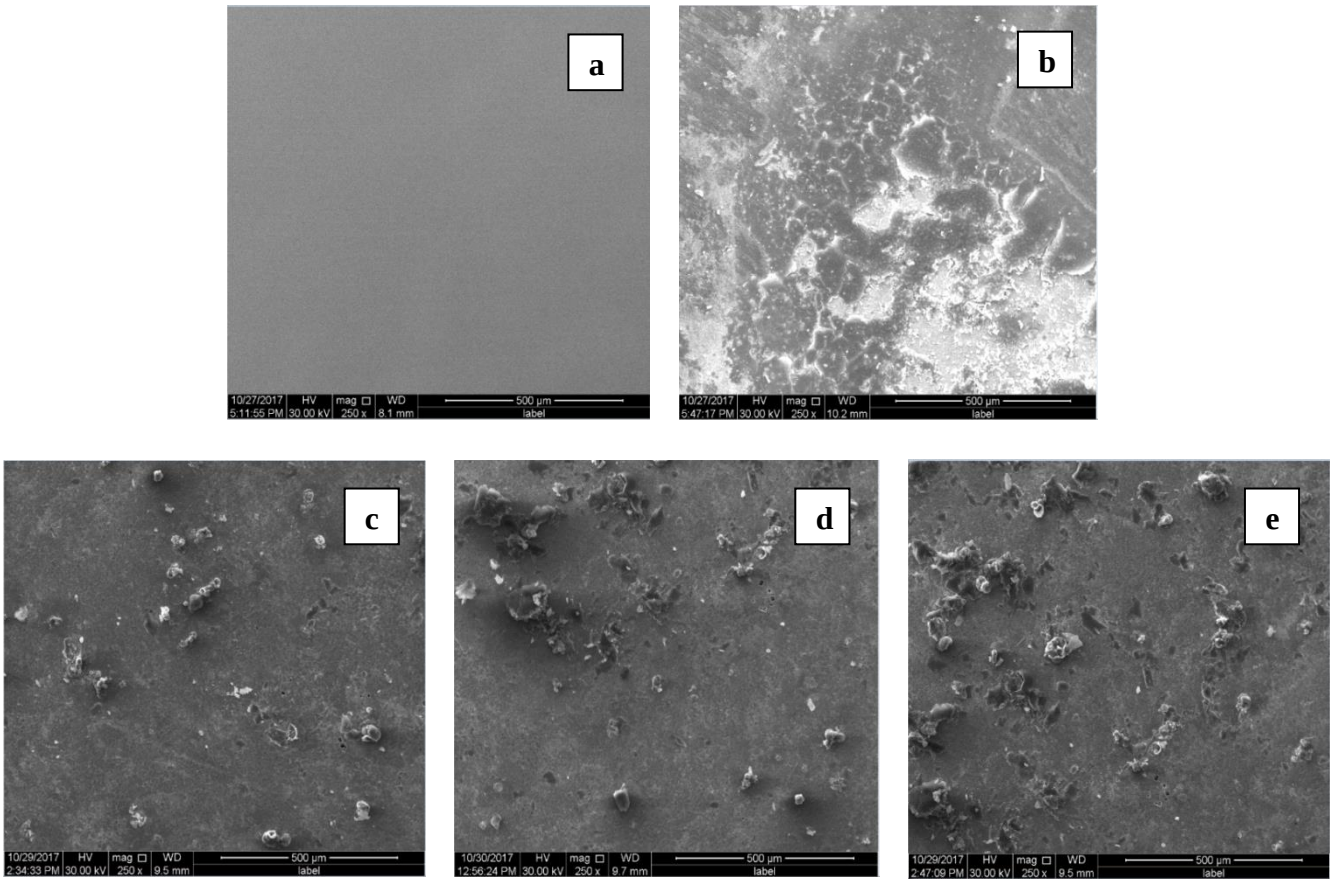

Figure 15(a-e): SEM micrographs of mild steel surface (a) before immersion in 0.5 M HCl, (b) after immersion in 0.5 M HCl for 12 h, (c, d and e) after 12 h of immersion in 0.5 M HCl + 900 ppm of the synthesized surfactants AS, HS and TS, respectively, at 25 °C.

3.5. Surface Investigations

Scanning electron microscopy (SEM) micrographs of mild steel samples in 0.5 M HCl in the absence and presence of 900 ppm of the investigated surfactants are shown in Figure 15(a–e). Figure 15a and b shows the pure mild steel surface before immersion in 0.5 M HCl and after immersion in 0.5 M HCl for 12 h, respectively. It can be observed from Figure 15b that the mild steel surface was strongly damaged due to the its exposure to the acid.

Figure 15(c–e) manifests SEM images of mild steel surface after treatment with 900 ppm of the synthesized surfactants AS, HS and TS, respectively, in the corrosive medium (0.5 M HCl). It is clear that, steel surface suffered a remarkable change from the previous case, and the strong damage shown in the steel surface was disappeared and the surface was largely covered with the surfactant inhibitors on the whole surface. This could be attributed to the strong adsorption of the inhibitors on the steel surface, causing a decrease in the contact between steel surface and corrosive medium, and thus exhibiting an excellent corrosion inhibition properties [61].

3.5. Mechanism of Corrosion Inhibition

From the experimental observations of the different employed methods it can be concluded that corrosion inhibition of mild steel in HCl solution by the synthesized surfactants were found to depend on the concentration and nature of the surfactant. The suggested inhibition mechanism involves adsorption of the surfactants on mild steel surface because such surfactants contain polar groups such as O and N and each atom is considered as an adsorption center and the extent of inhibition efficiency depends on the electron density around this center. These electrons interact with the vacant d-orbital of iron present in mild steel surface and adsorb strongly on the surface as illustrated in Fig. 16. Also, the higher values of % IE may be due to the higher number of carbon atoms of the hydrophobic tail which results in the increase in the electron density on the N and O atoms. On the other hand, the observed highest inhibition efficiency of the surfactant TS is due to the presence of indole moiety in its structure. The order of inhibition efficiency is as follows: TS > HS > AS.

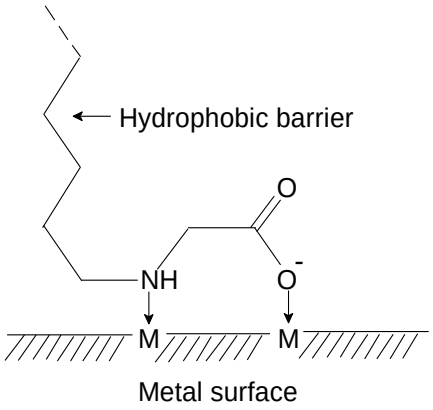

Figure 16. Suggested adsorption model of the synthesized amino acids-based surfactants on the mild steel surface.

3.6. Surface Active Properties

3.6.1. Surface Tension (γ)

A variation of the values of γ for different concentrations of the synthesized surfactants is represented in Fig. 17, and from which the critical micelle concentration (CMC) and the surface tension at CMC (γ_{CMC}) were evaluated. Sharp decreases in the values of γ with increasing concentration, then the curves break and continue to decrease slowly suggesting complete dissociation of the counter ion.

3.6.2. Critical Micelle Concentration(CMC)

The CMC is the main characteristic of any surfactant which is defined as the concentration above which surfactant molecules self-assemble into aggregates called micelles. The values of CMC were determined from the intersection points in the γ - log C curves [62] and are listed in Table 8. Such values demonstrate that the synthesized compounds are surfactants.

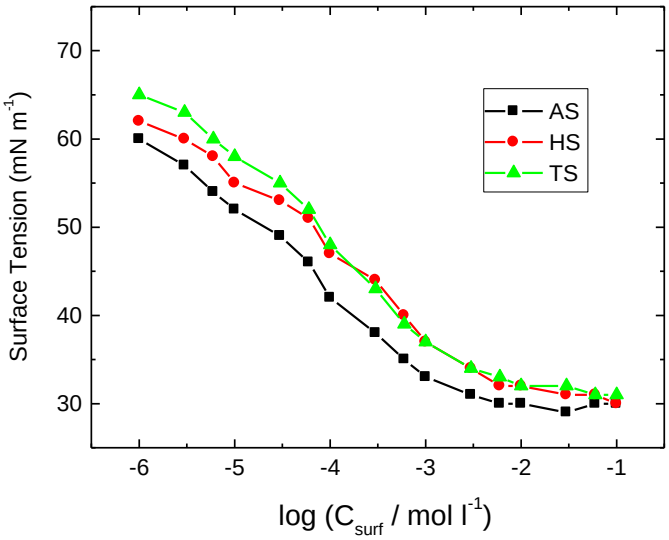

Figure 17. Surface tension versus logarithm concentration plots for the synthesized surfactants at 25°C

3.6.3. Effectiveness

Values of γ_{CMC} were used to calculate values of the surface pressure or effectiveness (Π_{CMC}) from the equation [63]:

$$\Pi_{CMC} = \gamma_0 - \gamma_{CMC} \quad (9)$$

where, γ_0 for pure water (72 $mN \cdot m^{-1}$ at 25 °C) and γ_{CMC} at CMC. Values of Π_{CMC} of the synthesized surfactants are inserted in Table 8. According to the results listed in Table 8, the synthesized surfactant AS is more effective than both HS and TS because it gave the greater lowering in γ_{CMC} than the others.

3.6.4. Maximum Surface Excess

Maximum surface excess of adsorbed surfactant molecules at the interface (Γ_{max}) is defined as the effectiveness of adsorption at an interface. Values of Γ_{max} of the synthesized surfactants (Table 8) were calculated using Gibbs adsorption equation [67]:

$$\Gamma_{max} = \frac{1}{2.303nRT}\left(\frac{\partial\gamma}{\partial \log C}\right) \quad (10)$$

where ($d\gamma/d$ log$C$) is the slopes of the straight lines in the surface tension plots and n is the number of species ions in solution.

3.6.5. Minimum Surface Area

Values of minimum surface area (A_{min}) (Table 8) were calculated according to the following equation [65]:

$$A_{min} = \frac{10^{16}}{N_A \Gamma_{max}} \quad (11)$$

where N_A is the Avogadro's number.

3.6.6. Cloud Point

The temperature at which the clear or nearly clear solution becomes definitely turbid is called cloud point. Cloud points were determined by raising the temperature of the surfactant solutions (0.1 M) in a controlled-temperature bath and cooling them until they become clear again. The synthesized surfactants were found to have high cloud points as listed in Table 8, which gave a good performance in hot water.

3.6.7. Foaming Height

Foaming properties were determined for 0.1 M surfactant solutions at 25 ^{o}C using a 100-ml graduated cylindrical column surrounded by a jacket so as to maintain the column at the desired temperature. A pipette was filled with the test solution and supported in the above column. The stop cock of the pipette was opened and the solution was allowed to fall into the same test solution in the column creating foam. Initial height and height after 5 minutes of foam were recorded on the scale attached to the column. The foaming height values for the surfactants revealed that the synthesized surfactants could be utilized as stable foaming agents.

3.6.8. Wetting Time

Determination of wetting times of the synthesized surfactants was carried out by immersing cotton skeins in their aqueous solutions (0.1 M) at 25 ^{o}C and recording the sinking times on the surfactant solutions taken in 500 ml measuring cylinders. These values are listed also in Table 8.

Table 8. Values of surface tension (γ), critical micelle concentration (CMC), surface tension at CMC (γ_{CMC}), effectiveness (Π_{CMC}), maximum surface excess (Γ_{max}), minimum surface area (A_{min}), cloud point (°C), foaming height (mm) and wetting time (sec) of the synthesized surfactants at 25 °C.

Inhibitor	γ mN m^{-1}	10^3 CMC (mol l^{-1})	γ_{CMC} mN m^{-1}	Π_{CMC} mN m^{-1}	10^{12} Γ_{max} mol cm^{-2}	10^3 A_{min} nm^2	Cloud Point (°C)	Foaming Height (mm)	Wetting Time (sec)
AS	45.6	13.2	29.3	42.7	10.2	1.62	79	167	127
HS	43.9	5.9	31.8	40.2	9.6	1.71	81	169	133
TS	42.4	4.8	33.1	38.9	9.4	1.77	84	175	129

3.6.9.The Relation between Corrosion Inhibition and Surface Properties of the Synthesized Surfactants

The suggested mechanism of corrosion inhibition of the synthesized surfactants depends on the ability of such surfactants to adsorb on the mild steel surface to form a protective layer. So, the CMC is very significant in determining the effectiveness of surfactants as corrosion inhibitors. Therefore, the surfactant TS which showed the lowest value of CMC (4.8×10^{-3}), it considered as the most effective corrosion inhibitor for mild steel. Also, values Γ_{max} of both AS and HS are higher than Γ_{max} of TS. On the other hand, A_{min} values of both AS and HS are lower than that of TS. The high value of A_{min} for TS and low value of Γ_{max} indicate more homogenous adsorbed film on the steel surface. All these parameters explain why TS is the most effective inhibitor.

4. CONCLUSIONS

1) The new synthesized amino acids-based surfactants (AS, HS and TS) act as good inhibitors for the corrosion of mild steel in HCl solutions.

2) The results obtained from polarization measurements revealed that synthesized surfactants behave as a mixed type inhibitors with anodic predominance.

3) Adsorption of synthesized surfactants on mild steel follows the Langmuir adsorption isotherms.

4) The obtained thermodynamic parameters for adsorption indicate that the adsorption process is spontaneous and endothermic, and the type of adsorption is physical.

5) Results obtained from all employed techniques are consistent with each others.

6) Surface active properties were evaluated which indicate that the synthesized compounds are good surfactants.

ACKNOWLEDGMENTS
The authors would like to thank the Deanship of Scientific Research at Umm Al-Qura University (Project code 15-SCI-3-1-0014) for the financial support.

References

1. M. Abdallah, O.A. Hazazi, A. Fawzy, S. El-Shafei and A.S. Fouda, *Prot. Met. Phys. Chem. Surf.,* 50 (2014) 659.
2. X. Li, S. Deng and H. Fu, *Corros. Sci.,* 55 (2006) 288.
3. M. Abdallah, B.H. Asghar, I. Zaafarany and A.S. Fouda, *Int. J. Electrochem. Sci.,* 7 (2012) 282.
4. M. Abdallah, I. Zaafarany, K.S. Khairou and M. Sobhi, *Int. J. Electrochem. Sci.,* 7 (2012) 1564.
5. M. Abdallah, M.M. Salem, B.A. AL-Jahdaly, M.I. Awad, E. Helal and A.S. Fouda, *Int. J. Electrochem Sci.,* 12 (2017) 4543.
6. M.I. Awad, A.F. Saad, M.R. Shaaban, B.A. AL-Jahdaly and O.A. Hazazi, *Int. J. Electrochem. Sci.,* 12 (2017) 1657.
7. O. A. Hazazi, A. Fawzy, M. R. Shaaban and M. I. Awad, *Int. J. Electrochem. Sci.*, 9, 1378 (2014).
8. M. Abdallah, A.S. Fouda, I. Zaafarany, A. Fawzy and Y. Abdallah, *J. Am. Sci.*, 9 (2013) 209.
9. O.A. Hazazi, A. Fawzy and M.I. Awad, *Chem. Sci. Rev. Lett.,* 4 (2015) 67.
10. M. Abdallah, M.M. Salem, A. Fawzy and A.A. Abdel Fattah, *J. Mater. Env. Sci.,* 8 (2017) 2599.
11. M. Abdallah, M.M. Salem, A. Fawzy and E.M. Mabrouk, *J. Mater. Env. Sci*., 8 (2017) 1320.
12. B. Gao, X. Zhang and Y. Sheng, *Mater. Chem. Phys*., 108 (2008) 375.
13. M. El Azhar, M. Traisnel, B. Mernari, L. Gengembre, F. Bentiss and M. Lagrenée, *Appl. Surf. Sci.,* 185 (2002) 197.
14. R. Karthikaiselvi, S. Subhashini and R. Rajalakshmi, *Arab. J. Chem*., 5 (2012) 517.
15. B. Qian, J. Wang, M. Zheng and B. Hou, *Corros. Sci.,* 75 (2013) 184.
16. M. Abdallah, H.M. Al-Tass, B.A. AL-Jahdaly and A.S. Fouda, *J. Mol. Liq.,* 216 (2016) 590.
17. M. Abdallah, S.T. Atwa I.A. Zaafarany, *Int. J. Electrochem. Sci.,* 9 (2014) 4747.
18. M. Abdallah B.A. AL-Jahdaly, M. Sobhi and A.I. Ali, *Int. J. Electrochem. Sci.*,10 (2015) 441.
19. O.A. Hazazi, A. Fawzy and M.I. Awad, *Int. J. Electrochem. Sci.,* 9 (2014) 4086.
20. M. Abdallah, H.E. Megahed and M.S. Motae, *Monats Chem.,* 141 (2010) 1287.
21. M. A. Malik, M. Al-Hashim, F. Nabi, S.A. Al-Thabiti, Z. Khan, *Int. J. Electrochem. Sci.,* 6 (2011) 1927.
22. K. Baczko, C. Larpenta and P. Lesot, *Tetrahed. Asym.*, 15 (2004) 971.
23. S.Y. Mhaskar, G. Lakshminarayana and L. Saisree, *J. Am. Oil Chem. Soc.,* 70 (1993) 23.
24. H. Yokota, K. Sagawa, C. Eguchi, M. Takehara, K. Ogino and T. Shibayama, *J. Am. Oil Chem. Soc.*, 62 (1985) 1716.
25. P. Clapes, M.R. Infante, *Biocat. Biotrans.,* 20 (2002) 215.
26. A. Nnanna, J. Xia, In *Protein Based Surfactants: Synthesis, Physicochemical Properties and Applications*; Surfactant Science Series Vol. 101 New York: Marcel Dekker, 2001.
27. D. Savage, G. Malone, S.R. Alley, J.F. Gallagher, A. Goel, P.N. Kelly, H.M. Bunz and P.T.M. Kenny, *J. Organomet. Chem.,* 691 (2006) 463.
28. A.M. Al-Sabagh, N.M. Nasser, O.E. El-Azabawy and A.E. El-Tabey, *J. Mol. Liq.,* 219 (2016) 1078.
29. J. Li, Y. Sha, *Molecules,* 13 (2008) 1111.
30. Y. Le, in "*Synthesis and physicochemical study of novel amino acid based surfactants*" Master Thesis, Göteborg, Sweden, p. 2, 2011.
31. L.B. Tang, G.N. Mu and G.H. Liu, *Corros. Sci.,* 45 (2003) 2251.
32. P. Manjula, S. Manonmani, P. Jayaram and S. Rajendran, *Anti-Corros. Methods Mater*., 48 (2001) 319.
33. H. Ma, S. Chen, L. Niu, S. Zhao, S. Li and D. Li, *J. Appl. Electrochem.*, 32 (2002) 65.
34. M. Bjelopavlic, J. Ralston and G. Reynolds, *J. Coll. Int. Sci.*, 208 (1998) 183.
35. M.A. Deyab, *Corros. Sci.,* 49 (2007) 2315.
36. T.P. Zhao and G.N. Mu, *Corros. Sci.*, 41 (1999) 1937.
37. F. Touhami, A. Aouniti, Y. Abed, B. Hammouti, S. Kertit, A. Ramdani and K. Elkacemi, *Corros. Sci.,* 42 (2000) 929.

38. M. Christov and A. Popova, *Corros. Sci.*, 46 (2004) 1613.
39. S.K. Shukla and M.A. Quraishi, *Corros. Sci.*, 51 (2009) 1007.
40. P.C. Okafor, Y. Zheng, *Corros. Sci*., 51 (2009) 850.
41. M. Behpour, S.M. Ghoreishi, N. Soltani, M. Salavati-Niasari, M. Hamadanian and A. Gandomi, *Corros. Sci.*, 50 (2008) 2172.
42. L.B. Tang, G.N. Mu and G.H. Liu, *Corros. Sci.*, 45 (2003) 2251.
43. F. Bentiss, M. Traisnel and M. Lagrenee, *Corros Sci.*, 42 (2000) 127.
44. K.F. Khaled, *J. Appl. Electrochem*., 39 (2009) 429
45. W. Durnie, R.D. Marco, A. Jefferson and B. Kinsella, *J. Electrochem Soc.*, 146 (1999) 1751.
46. M. Elachouri, M.S. Hajji, M. Salem, S. Kertit, J. Aride, R. Coudert and E. Essassi, *Corrosion*, 52 (1996) 103.
47. R. Solmaz, *Corros Sci*., 79 (2014) 169.
48. X. Li, S. Deng, H. Fu and T. Li, *Electrochim Acta*, 54 (2009) 4089.
49. B. Xu, Y. Liu, X. Yin, W. Yang and Y. Chen, *Corros. Sci.*, 74 (2013) 206.
50. A. Anejjar, A. Zarrouk, R. Salghi, H. Zarrok, D. Ben Hmamou, B. Hammouti, B. Elmahi and S.S. Al-Deyab, *J. Mater. Env. Sci.*, 4 (2013) 583.
51. J.O.M. Bockris and A.K.N. Reddy, *Modern Electrochemistry*, Vol. 2, Plenum Press, New York, 1977.
52. J. Marsh, *Advanced Organic Chemistry*, 3rd ed., Wiley, Eastern New Delhi, 1988.
53. U.R. Evans, *The Corrosion of Metals*, Edward Arnold, London, 1960. p. 898.
54. T.Y. Soror and M.A. El-Ziady, *Mater. Chem. Phys.*, 77 (2002) 697.
55. M.A. Amin and K.F. Khaled, *Corros. Sci.*, 52 (2010) 1762.
56. G.N. Mu, X.H. Li, Q. Qu and J. Zhou, *Corros. Sci.*, 48 (2006) 445.
57. G. Trabanelli, C. Montecelli, V. Grassi and A. Frignani, *J. Cem. Concr. Res.*, 35 (2005) 1804.
58. F.M. Reis, H.G. De Melo and I. Costa, *Electrochim. Acta*, 51 (2006) 17.
59. M.A. Quraishi and J. Rawat, *Mater. Chem. Phys.*, 70 (2001) 95.
60. C. Hsu, F. Mansfeld, *Corrosion*, 57 (2001) 747.
61. R. Prabhu, T. Venkatesha, A. Shanbhag, G. Kulkarni and R. Kalkhambkar, *Corros. Sci.*, 50 (2008) 3356.
62. D.P. Schweinsberg, A.G. George, A.K. Nanayakkara and D.A. Steinert, *Corros. Sci.*, 28 (1988) 87.
63. K.F. Khaled and N. Hackerman, *Electrochim. Acta*, 48 (2003) 2715.
64. F.K.G. Santos, E.L.B. Neto, M.C.P. Moura, T.N.C. Dantas and A.A.D. Neto, *J. Coll. Surf. A: Physicochem. Eng. Asp.*, 333 (2009) 156.
65. C. Gamboa, A.F. Olea and C. Gamboa, *J. Coll. Surf. A: Physicochem. Eng. Asp.*, 278 (2006) 241.